In situ electric-field control of THz nonreciprocal directional dichroism in the multiferroic Ba2CoGe2O7

J. Vít, J. Viirok, L. Peedu, T. Rõõm, U. Nagel, V. Kocsis, Y. Tokunaga, Y. Taguchi, Y. Tokura, István Kézsmárki, P. Balla, K. Penc, J. Romhányi, S. Bordács

Angaben zur Veröffentlichung / Publication details:

Vít, J., J. Viirok, L. Peedu, T. Rõõm, U. Nagel, V. Kocsis, Y. Tokunaga, et al. 2021. "In situ electric-field control of THz nonreciprocal directional dichroism in the multiferroic Ba2CoGe2O7." *Physical Review Letters* 127 (15): 157201. https://doi.org/10.1103/physrevlett.127.157201.

In Situ Electric-Field Control of THz Nonreciprocal Directional Dichroism in the Multiferroic $Ba_2CoGe_2O_7$

J. Vít,[1,2,3] J. Viirok,[4] L. Peedu,[4] T. Rõõm,[4] U. Nagel,[4] V. Kocsis,[5] Y. Tokunaga,[5,6] Y. Taguchi,[5] Y. Tokura,[5,7] I. Kézsmárki,[1,8] P. Balla,[9] K. Penc,[9] J. Romhányi,[10] and S. Bordács[1,11]

[1]*Department of Physics, Budapest University of Technology and Economics, 1111 Budapest, Hungary*
[2]*Institute of Physics ASCR, Na Slovance 2, 182 21 Prague 8, Czech Republic*
[3]*Faculty of Nuclear Science and Physical Engineering, Czech Technical University, Břehová 7, 115 19 Prague 1, Czech Republic*
[4]*National Institute of Chemical Physics and Biophysics, Akadeemia tee 23, 12618 Tallinn, Estonia*
[5]*RIKEN Center for Emergent Matter Science (CEMS), Wako 351-0198, Japan*
[6]*Department of Advanced Materials Science, University of Tokyo, Kashiwa 277-8561, Japan*
[7]*Department of Applied Physics and Tokyo College, University of Tokyo, Tokyo 113-8656, Japan*
[8]*Experimental Physics V, Center for Electronic Correlations and Magnetism, University of Augsburg, 86135 Augsburg, Germany*
[9]*Institute for Solid State Physics and Optics, Wigner Research Centre for Physics, P.O. Box. 49, H-1525 Budapest, Hungary*
[10]*Department of Physics and Astronomy, University of California, Irvine, 4129 Frederick Reines Hall, Irvine, California 92697, USA*
[11]*Hungarian Academy of Sciences, Premium Postdoctor Program, 1051 Budapest, Hungary*

(Received 26 January 2021; accepted 28 July 2021; published 5 October 2021)

Nonreciprocal directional dichroism, also called the optical-diode effect, is an appealing functional property inherent to the large class of noncentrosymmetric magnets. However, the *in situ* electric control of this phenomenon is challenging as it requires a set of conditions to be fulfilled: Special symmetries of the magnetic ground state, spin excitations with comparable magnetic- and electric-dipole activity, and switchable electric polarization. We demonstrate the isothermal electric switch between domains of $Ba_2CoGe_2O_7$ possessing opposite magnetoelectric susceptibilities. Combining THz spectroscopy and multiboson spin-wave analysis, we show that unbalancing the population of antiferromagnetic domains generates the nonreciprocal light absorption of spin excitations.

DOI: 10.1103/PhysRevLett.127.157201

The interaction between light and matter may produce fascinating phenomena. Among them is the nonreciprocal directional dichroism (NDD), when the absorption differs for the propagation of light along and opposite to a specific direction. In contrast to the magnetic circular dichroism, the absorption difference for NDD is finite even for unpolarized light. The chirality of the light lies at the heart of the phenomenon: the electric ($\mathbf{E}^\omega$) and magnetic ($\mathbf{H}^\omega$) field components of the light and its propagation vector $\mathbf{k} \propto \mathbf{E}^\omega \times \mathbf{H}^\omega$ form a right-handed system. Applying orthogonal static electric ($\mathbf{E}$) and magnetic ($\mathbf{H}$) fields to a material breaks the inversion and time-reversal symmetries, leading to the observation of NDD [1]. Such a symmetry breaking is inherent to magnetoelectric (ME) multiferroics, materials with coexisting electric and magnetic orders. In multiferroics, the ME coupling establishes a connection between responses to electric and magnetic fields: an external electric field generates magnetization $\mathbf{M}$, and a magnetic field induces electric polarization $\mathbf{P}$ in the sample. The NDD is manifested by the refractive index difference $\Delta N = N_+ - N_-$ for counterpropagating ($\pm\mathbf{k}$) linearly polarized beams [2–4]. In the long-wavelength limit,

$$N_\pm = \sqrt{\varepsilon_{\alpha\alpha}\mu_{\beta\beta}} \pm \chi^{em}_{\alpha\beta}, \tag{1}$$

where $\varepsilon_{\alpha\alpha}$ and $\mu_{\beta\beta}$ are the components of the permittivity and the permeability tensors for oscillating fields polarized along E^ω_α and H^ω_β, and $\chi^{em}_{\alpha\beta}$ is the ME susceptibility characterizing the induced polarization $\delta P^\omega_\alpha \propto \chi^{em}_{\alpha\beta} H^\omega_\beta$. The $\chi^{em}_{\alpha\beta}$ becomes resonantly enhanced for spin excitations of multiferroics endowed with a mixed magnetic and electric dipole character giving rise to strong NDD [2–9].

Since $\Delta N \propto \chi^{em}_{\alpha\beta}$, the absorbing and transparent directions are determined by the sign of ME susceptibility, and therefore, they can be interchanged by the sign reversal of the $\chi^{em}_{\alpha\beta}$. The magnetic field can naturally switch between time-reversed magnetic states with opposite signs of ME responses, and allows the control of NDD [2–4]. Can we achieve a similar switch with an electric field, which is a time-reversal even quantity? Apart from being a fundamental question, the voltage control of NDD may promote the application of multiferroics in GHz–THz frequency data transmission and signal processing devices with reduced size and energy consumption. In addition to the

NDD, the electric-field-induced switching between time-reversed magnetic states would also provide an efficient way to control other optical ME effects, such as chirality of magnons [3,10,11] or axion-term-induced gyrotropy [12]. The ME coupling may help us to achieve the desired control of magnetic states [5,7,13–16], however, realizing this effect is not at all trivial. It requires a magnetic order permitting NDD and a polarization that is switchable by laboratory electric fields. In the visible spectral range, the realization of this effect has been confirmed for charge excitations [14,15]. However, studies in the THz range of spin-wave excitations are scarce. So far, mostly ME poling was used to select between time-reversed domains by cooling the sample through the ordering temperature in external magnetic and electric fields [5,7,16]. The electric field induced changes in the absorption coefficient were detected only recently [17].

In this Letter, we demonstrate the isothermal electric field control of the THz frequency NDD in $Ba_2CoGe_2O_7$, which provides an ideal model system due to its simple antiferromagnetic (AFM) order. The electric field switches between the transparent and absorbing directions, where the absorption difference between the two is experimentally found as high as 30%. We attribute the observed change of the NDD to the electric-field-induced imbalance in the population of the AFM domains.

The discovery of the ME properties of $Ba_2CoGe_2O_7$ [18], followed by a detection of the gigantic ME effect in $Ca_2CoSi_2O_7$ [19] aroused interest in this family of quasi-two-dimensional compounds. They crystallize in the noncentrosymmetric $P\bar{4}2_1m$ structure, where the unit cell includes two spin-3/2 magnetic Co^{2+} ions, as shown in Fig. 1(a). Below $T_N = 6.7$ K, the spins order in a two-sublattice easy-plane AFM structure [20]. A small in-plane anisotropy pins the AFM ordering vector $\mathbf{L} = \mathbf{M}_A - \mathbf{M}_B$ to one of the symmetry-equivalent $\langle 100 \rangle$ directions of the tetragonal plane, as shown in Fig. 1 [21–23]. Applying an external magnetic field $\mathbf{H} \| [110]$ rotates the $\mathbf{L}$ vector to $[1\bar{1}0]$, and gives rise to a sizeable ferroelectric polarization $\mathbf{P}$ along the tetragonal [001] axis [24]. The same ME interaction leads to NDD for the THz spin excitations of $Ba_2CoGe_2O_7$ [25,26], which has been observed for in-plane magnetic fields: (i) for light propagation $\mathbf{k}$ along the cross product of the magnetic field $\mathbf{H} \| [110]$ and the magnetic-field-induced polarization $\mathbf{P} \| [001]$ [2,4], and (ii) for $\mathbf{k} \| \mathbf{H} \| [100]$ when a chiral state is realized [3].

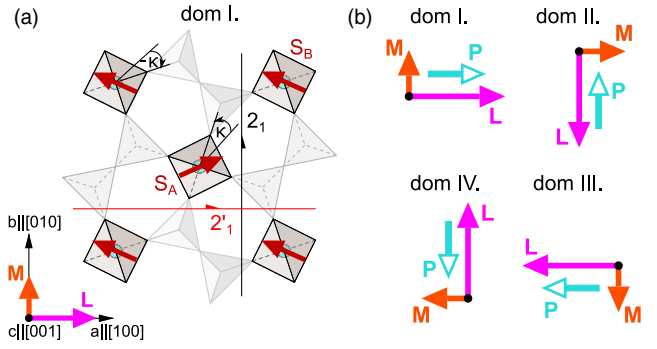

FIG. 1. (a) The canted antiferromagnetic order of $Ba_2CoGe_2O_7$ in domain I in zero fields. Cyan circles denote the Co^{2+} ions with $S = 3/2$ (dark red arrows) in the center of the O^{2-} tetrahedra (grey). The symmetry operations are the 2_1 screw axis, (black half-arrow) and the orthogonal $2'_1$ screw axis followed by the time reversal (red half-arrow). $\mathbf{M}$ and $\mathbf{L}$ correspond to the uniform and staggered sublattice magnetizations, respectively. (b) The four antiferromagnetic domains. A magnetic field applied along the [001] axis induces a polarization $\delta\mathbf{P}$ (light blue arrows) via linear magnetoelectric effect.

Both the static and the dynamic ME response of $Ba_2CoGe_2O_7$ are consistently explained by the spin-dependent p–d hybridization [24–28]. In this mechanism, the spin-quadrupole operators of the $S = 3/2$ cobalt spin directly couple to the induced polarization $\mathbf{P}_j$,

$$\begin{aligned} P_j^a &\propto -\cos 2\kappa_j (S_j^b S_j^c + S_j^c S_j^b) + \sin 2\kappa_j (S_j^a S_j^c + S_j^c S_j^a), \\ P_j^b &\propto -\cos 2\kappa_j (S_j^a S_j^c + S_j^c S_j^a) - \sin 2\kappa_j (S_j^b S_j^c + S_j^c S_j^b), \\ P_j^c &\propto -\cos 2\kappa_j (S_j^a S_j^b + S_j^b S_j^a) + \sin 2\kappa_j [(S_j^a)^2 - (S_j^b)^2], \end{aligned} \tag{2}$$

where j is the site index, and a, b, c are parallel to [100], [010], and [001], respectively. $\kappa_j = \kappa$ in A sublattice and $\kappa_j = -\kappa$ in B sublattice account for the different orientation of the tetrahedra [see Fig. 1(a)]. The same mechanism is the source of the multiferroic properties of $Sr_2CoSi_2O_7$ [29], the observation of spin-quadrupolar excitations in $Sr_2CoGe_2O_7$ in the field aligned phase [30], and the microwave nonreciprocity of magnons in $Ba_2MnGe_2O_7$ [31].

The clue how to control the NDD using electric fields comes from the experiment of Murakawa *et al.* [24]. They showed that a magnetic field applied nearly parallel to the tetragonal axis induces an in-plane electric polarization along one of the $\langle 100 \rangle$ directions. The hysteresis of the polarization observed upon tilting the field away from the [001] axis suggests a rearrangement of the magnetic domain population. The AFM order reduces the space group symmetry from $P\bar{4}2_1m1'$ to $P2'_12_12'$, corresponding to the breaking of the rotoreflection symmetry $\bar{4}$, and the formation of four magnetic domains, shown in Fig. 1(b) [32]. The $P2'_12_12'$ symmetry gives rise to a finite χ^{em}, and in a magnetic field $\mathbf{H} \| [001]$, a polarization $\delta\mathbf{P}$ parallel to the $\mathbf{L}$ develops, as shown in Fig. 1(b). If the field is perfectly aligned $\mathbf{H} \| [001]$, the four domains remain equivalent and the field-induced polarizations $\delta\mathbf{P}$ cancel out. However, a small perturbation such as tilting of the magnetic field or applying an in-plane electric field can break the delicate balance between the domains. In our experiments, we exploit this highly susceptible state to

change the relative population of the domains by electric field, $\mathbf{E}\|[100]$, and attain control over the NDD, present for $\mathbf{k}\|\mathbf{E}\times\mathbf{H}$.

$Ba_2CoGe_2O_7$ single crystals were grown by the floating zone technique as described in [24]. Silver paste electrodes were painted on the parallel sides of a $2\times3\times0.7$ mm^3 rectangular (010) cut. The THz spectra were measured in Tallinn with a Martin-Puplett interferometer and a 0.3 K silicon bolometer. We applied the external magnetic and electric fields in the $\mathbf{H}\|[001]$ and $\mathbf{E}\|[100]$ directions, while the THz radiation propagated along the $\mathbf{k}\|[010]$ axis. The crystallographic axes of the sample were oriented by x-ray Laue diffraction and aligned in the THz experiment to, at least, 1° precision. The THz absorption spectra were deduced as described in Ref. [33].

Our main experimental results are summarized in Fig. 2. Panel 2(a) displays the average and 2(b) the difference of the THz absorption spectra measured in electric fields with opposite signs ($E=\pm3$ kV/cm) and constant magnetic fields. In agreement with former results [26], we assign the absorption peak around 18 cm^{-1} (mode No. 1) to the optical magnon excitation of the easy-plane AFM ground state, whereas resonances No. 2, No. 3, and No. 4, showing a V shape splitting in magnetic fields, are attributed to the spin stretching modes involving the modulation of the spin length. In a finite magnetic field, the absorption spectra become different for the opposite signs of the electric field as evidenced by Fig. 2(b) for the light polarization $\mathbf{E}^\omega\|[001]$ and $\mathbf{H}^\omega\|[100]$. The electric field odd component of the signal is the manifestation of the NDD, and it shows that the absorption is different for light propagation along or opposite to the cross product of the static electric and magnetic fields $\mathbf{E}\times\mathbf{H}$. This relation is further supported by the fact that the differential absorption spectra change sign under the reversal of the external magnetic field. The NDD is finite only for the spin stretching modes No. 2 and No. 3 and it increases with magnetic fields up to ~12 T. We note that, for the orthogonal light polarization, $\mathbf{E}^\omega\|[100]$ and $\mathbf{H}^\omega\|[001]$, we did not find electric-field-induced absorption difference within the accuracy of the experiment.

The electric-field-induced change in the absorption spectra around mode No. 3, measured with respect to the zero-field-cooled state, is displayed in Fig. 3(a). The peak absorption, shown in Fig. 3(b), depends on the electric field history of the sample: the initial and the following upward and downward sweeps are all different, and the absorption difference has a small but finite remanence [34]. Furthermore, the electric field can change the absorption only below T_N as displayed in Fig. 3(c), though the intensity of the spin stretching mode remains finite even above T_N [2]. All of these findings suggest that the observed electric field effect arises only in the magnetically ordered phase, and it is related to switching between domain states possessing different NDD.

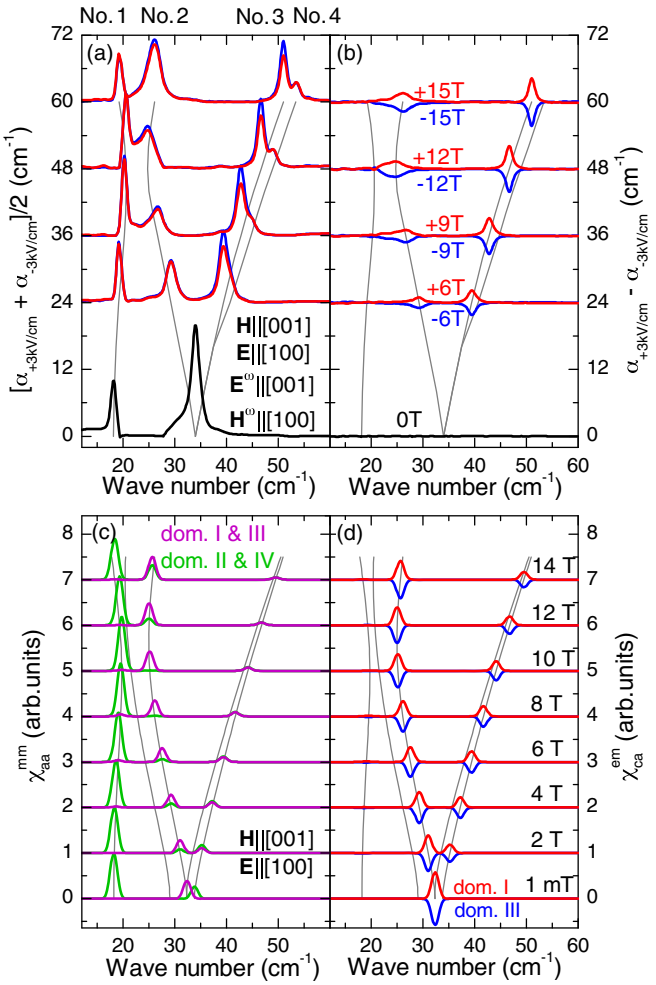

FIG. 2. (a) Magnetic field dependence of the THz absorption spectra averaged for the measurements performed in electric fields with opposite signs, $E=\pm3$ kV/cm at $T=3.5$ K. The light polarization is $\mathbf{E}^\omega\|[001]$ and $\mathbf{H}^\omega\|[100]$. The spectra measured in positive (red) or negative (blue) magnetic fields $\mathbf{H}\|[001]$ are shifted in proportion with the absolute value of the field. Grey lines indicate the magnetic field dependence of the resonance energies (peak Nos. 1–4). (b) shows the electric field-induced change in the absorption spectra as the difference of the absorption spectra recorded in $E=\pm3$ kV/cm. (c) The magnetic susceptibility calculated from the spin-wave theory in domains I and III (purple) and in domains II and IV (green). (d) The ME susceptibility in domain I (red) and domain III (blue).

Considering the symmetries of the zero-field ground state shown in Fig. 1(a), the (unitary) 2_1 screw axis restricts NDD for light propagation $\mathbf{k}\|\mathbf{c}\times\mathbf{L}$ in a given domain. When a magnetic field is applied along $\mathbf{H}\|[001]$, only the $2_1'$ symmetry remains. The S^b, S^c, P^a operators are even, while S^a, P^b, P^c are odd under $2_1'$ in domain I, depicted in Fig. 1(a). Since time reversal makes this symmetry anti-unitary, the operators are either even or odd under conjugation, restricting the transition matrix elements to be either real or imaginary [34,35]. As a consequence, the real part of a ME susceptibility combined from an even and odd

operator vanishes, annulling the time-reversal odd part of χ^{em}_{bc} and χ^{em}_{cb}, thus, forbidding NDD in domain I when $\mathbf{k}\|[100]$. The $2'_1$ does not affect NDD in the other propagation directions, and indeed, this is what we observed for $\mathbf{k}\|[010]$. In finite fields, we also expect NDD for the $\mathbf{k}\|[001]$—but then, the analysis of results would be more complicated as the Faraday effect mixes the polarization states of the light.

In order to interpret the experimental results quantitatively, we considered the microscopic Hamiltonian of interacting $S = 3/2$ Co^{2+} spins following Refs. [25,26]

$$\mathcal{H} = \sum_{\langle i,j\rangle}[J(\hat{S}^a_i\hat{S}^a_j + \hat{S}^b_i\hat{S}^b_j) + J^c\hat{S}^c_i\hat{S}^c_j] + \sum_i \Lambda(\hat{S}^c_i)^2 - \sum_i [g_{cc}H_c\hat{S}^c_i + E_a\hat{P}^a_i], \quad (3)$$

where summation $\langle i, j\rangle$ runs over the nearest neighbors. Beside the anisotropic exchange coupling (J and J^c), single-ion anisotropy Λ, and the Zeeman term, we introduce the coupling between the external electric field, E_a, and the spin-induced polarization [see Eq. (2)], which breaks the O(2) symmetry of the model.

We calculated the excitations above a variational site-factorized ground state using a multiboson spin-wave theory, following Ref. [26]. The approximate O(2) symmetry of the Hamiltonian (even for finite H_c) is reflected in the ground state manifold, the application of a tiny $E_a > 0$ combined with $H_c > 0$ selects domain I in Fig. 1(b), while $E_a < 0$ selects domain III as the variational ground state. We note that, even in the highest fields, the ME energy [24] is at least an order of magnitude smaller than the in-plane anisotropy [22], thus, the rotation of the AFM vector $\mathbf{L}$ away from the principal axes is negligible (e.g., [23]). The magnetic dipole strengths of the excitations are estimated by the transition matrix elements of the spin operators $|\langle 0|\hat{S}^\alpha|n\rangle|^2$ between the ground state $|0\rangle$ and the excited states $|n\rangle$. The contribution of the magnetic dipole processes to the absorption is shown in Fig. 2(c). The electric dipole matrix elements are evaluated similarly for polarization components $\hat{P}^\beta$. The ME susceptibility, $\chi^{em}_{ca} \propto \langle 0|P_c|n\rangle\langle n|S_a|0\rangle$ is plotted in Fig. 2(d).

For light polarization $\mathbf{E}^\omega\|[001]$ and $\mathbf{H}^\omega\|[100]$, our model predicts that two spin stretching modes have finite ME susceptibility χ^{em}_{ca} and, correspondingly, show NDD with the same sign. The overall sign of the ME response is reversed upon the reversal of either the static electric or the magnetic field related to the switching from domain I to III. All of these findings are in agreement with the experiments and imply that the electric field control of the NDD is realized by influencing the AFM domains. We note that, among modes No. 3 and No. 4, which show a tiny splitting in high fields, resonance No. 3 is NDD active in the experiment, whereas our theory predicts NDD for the higher energy mode. However, we found no obvious way to reproduce the fine structure of the resonance energies within our model or by including other realistic terms [21,24,25].

Although theory predicts that individual domains possess a finite dichroism as $H_c \to 0$ [see Fig. 3(b)], we observed vanishing NDD in this limit. This suggests that domain walls relax toward their initial positions, and the domain population evens out as fields go to zero. The multidomain state may be favored by: (i) electric dipole-dipole interaction between the ferroelectric domains; (ii) elastic energy, since the AFM domains break the tetragonal symmetry, they can couple to orthorhombic distortion [36]. The finite intensity of mode No. 1 also indicates that domains II and IV coexist with domains I and III. In domains I and III, excitation No. 1 is silent for this light polarization according to the calculation, since it can only be excited by the $\mathbf{H}^\omega\|[010]$, which is perpendicular to $\mathbf{L}\|[100]$. The polarization matrix element is also negligible for this resonance. Therefore, domains II and IV with finite magnetic dipole strength for $\mathbf{H}^\omega\|[100]$ [see Fig. 2(c)] should also be present in the studied sample. Thus, one expects even stronger NDD than observed experimentally here, if the monodomain state of either domain I or domain III can be realized. Finally, we note that the small difference in the averaged absorption [Fig. 2(a)] observed for the reversal of the magnetic field is probably caused by a small misalignment. When the magnetic field is

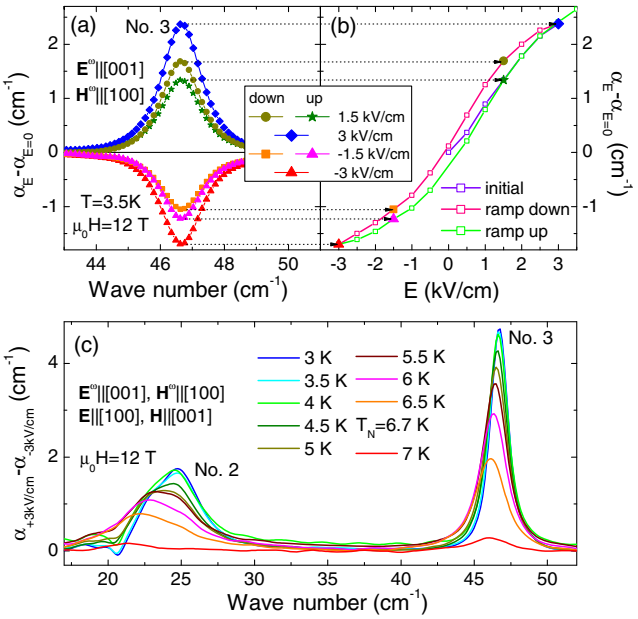

FIG. 3. (a) The electric field induced change in the absorption spectra measured with respect to the zero field cooled state at 3.5 K and in fixed magnetic field 12 T. (b) The hysteresis of the electric field dependence of the peak absorption. The horizontal arrows connect corresponding points of panels (a) and (b). (c) Temperature dependence of the electric field induced change in the absorption spectra measured in 12 T.

slightly tilted toward the light propagation $\mathbf{k}\|[010]$, the balance between domains I and III can be broken.

The absence of the NDD for the orthogonal light polarization, $\mathbf{E}^{\omega}\|[100]$ and $\mathbf{H}^{\omega}\|[001]$, can be explained by the smallness of the χ^{em}_{ac}. Because of the nearly preserved O(2) symmetry of the system, the magnetic matrix element in χ^{em}_{ac} involves the $\hat{S}^{c}$, which commutes with the terms of the Hamiltonian in Eq. (3) except for the $\mathbf{E}\cdot\mathbf{P}$. Therefore, the dipole oscillator strength for S^{c}—given by the double commutator [37]—is tiny compared to other matrix elements.

In summary, we demonstrated the isothermal voltage control of the nonreciprocal THz absorption in $Ba_2CoGe_2O_7$. In contrast to former studies applying ME poling, here, the ME polarization is induced by a magnetic field preserving the nearly O(2) symmetric ground states. The degeneracy within this manifold allows efficient voltage control of the magnetic domain population and, so, of the NDD. A similar mechanism may give rise to NDD in ME spin-spiral compounds, e.g., Cu_2OSeO_3 or $CoCr_2O_4$ with multidomain states. Our results can promote the applications of multiferroics in voltage-controlled high-frequency devices and stimulate search for compounds with stronger remanence and higher ordering temperatures.

The authors thank M. Mostovoy for enlightening discussions and K. Amelin for technical help. This research was supported by the Estonian Ministry of Education and Research Grants No. IUT23-3 and No. PRG736, by the European Regional Development Fund Project No. TK134, by the bilateral program of the Estonian and Hungarian Academies of Sciences under Contract No. NMK2018-47, by the Hungarian National Research, Development and Innovation Office NKFIH Grants No. ANN 122879 and No. K 124176, and by the Hungarian Eötvös Lóránd Research Network. The research reported in this Letter and carried out at the BME (Budapest University of Technology and Economics) has been supported by the NRDI Fund (TKP2020 IES, Grant No. BME-IE-NAT) based on the charter of bolster issued by the NRDI Office under the auspices of the Ministry for Innovation and Technology. J. V. was partially supported by the Grant Agency of the Czech Technical University in Prague (Project No. SGS19/188/OHK4/3T/14) and by the Project SOLID21 (Project No. CZ.02.1.01/0.0/0.0/16 019/0000760).

Note added.—During the preparation of this manuscript, we become aware of the related work of Kimura *et al.*, who study the electric field control of microwave NDD of the triplet Bose-condensate in $TlCuCl_3$ [38].

[1] G. L. J. A. Rikken, C. Strohm, and P. Wyder, Phys. Rev. Lett. **89**, 133005 (2002).
[2] I. Kézsmárki, N. Kida, H. Murakawa, S. Bordács, Y. Onose, and Y. Tokura, Phys. Rev. Lett. **106**, 057403 (2011).
[3] S. Bordács, I. Kézsmárki, D. Szaller, L. Demkó, N. Kida, H. Murakawa, Y. Onose, R. Shimano, T. Rõõm, U. Nagel, S. Miyahara, N. Furukawa, and Y. Tokura, Nat. Phys. **8**, 734 (2012).
[4] I. Kézsmárki, D. Szaller, S. Bordács, V. Kocsis, Y. Tokunaga, Y. Taguchi, H. Murakawa, Y. Tokura, H. Engelkamp, T. Rõõm, and U. Nagel, Nat. Commun. **5**, 3203 (2014).
[5] Y. Takahashi, R. Shimano, Y. Kaneko, H. Murakawa, and Y. Tokura, Nat. Phys. **8**, 121 (2012).
[6] D. Szaller, S. Bordács, V. Kocsis, T. Rõõm, U. Nagel, and I. Kézsmárki, Phys. Rev. B **89**, 184419 (2014).
[7] S. Kibayashi, Y. Takahashi, S. Seki, and Y. Tokura, Nat. Commun. **5**, 4583 (2014).
[8] A. M. Kuzmenko, V. Dziom, A. Shuvaev, A. Pimenov, M. Schiebl, A. A. Mukhin, V. Y. Ivanov, I. A. Gudim, L. N. Bezmaternykh, and A. Pimenov, Phys. Rev. B **92**, 184409 (2015).
[9] S. Yu, B. Gao, J. W. Kim, S.-W. Cheong, M. K. L. Man, J. Madéo, K. M. Dani, and D. Talbayev, Phys. Rev. Lett. **120**, 037601 (2018).
[10] A. M. Kuzmenko, A. Shuvaev, V. Dziom, A. Pimenov, M. Schiebl, A. A. Mukhin, V. Y. Ivanov, L. N. Bezmaternykh, and A. Pimenov, Phys. Rev. B **89**, 174407 (2014).
[11] R. Masuda, Y. Kaneko, Y. Tokura, and Y. Takahashi, Science **372**, 496 (2021).
[12] T. Kurumaji, Y. Takahashi, J. Fujioka, R. Masuda, H. Shishikura, S. Ishiwata, and Y. Tokura, Phys. Rev. Lett. **119**, 077206 (2017).
[13] B. B. Krichevtsov, V. V. Pavlov, and R. V. Pisarev, Pis'ma Zh. Eksp. Teor. Fiz. **44**, 471 (1986) [JETP Lett. **44**, 607 (1986)].
[14] M. Saito, K. Ishikawa, S. Konno, K. Taniguchi, and T. Arima, Nat. Mater. **8**, 634 (2009).
[15] T. Sato, N. Abe, S. Kimura, Y. Tokunaga, and T.-h. Arima, Phys. Rev. Lett. **124**, 217402 (2020).
[16] V. Kocsis, K. Penc, T. Rõõm, U. Nagel, J. Vít, J. Romhányi, Y. Tokunaga, Y. Taguchi, Y. Tokura, I. Kézsmárki, and S. Bordács, Phys. Rev. Lett. **121**, 057601 (2018).
[17] A. M. Kuzmenko, D. Szaller, T. Kain, V. Dziom, L. Weymann, A. Shuvaev, A. Pimenov, A. A. Mukhin, V. Y. Ivanov, I. A. Gudim, L. N. Bezmaternykh, and A. Pimenov, Phys. Rev. Lett. **120**, 027203 (2018).
[18] H. T. Yi, Y. J. Choi, S. Lee, and S.-W. Cheong, Appl. Phys. Lett. **92**, 212904 (2008).
[19] M. Akaki, J. Tozawa, D. Akahoshi, and H. Kuwahara, Appl. Phys. Lett. **94**, 212904 (2009).
[20] A. Zheludev, T. Sato, T. Masuda, K. Uchinokura, G. Shirane, and B. Roessli, Phys. Rev. B **68**, 024428 (2003).
[21] J. Romhányi, M. Lajkó, and K. Penc, Phys. Rev. B **84**, 224419 (2011).
[22] M. Soda, M. Matsumoto, M. Månsson, S. Ohira-Kawamura, K. Nakajima, R. Shiina, and T. Masuda, Phys. Rev. Lett. **112**, 127205 (2014).
[23] M. Soda, S. Hayashida, B. Roessli, M. Månsson, J. S. White, M. Matsumoto, R. Shiina, and T. Masuda, Phys. Rev. B **94**, 094418 (2016).
[24] H. Murakawa, Y. Onose, S. Miyahara, N. Furukawa, and Y. Tokura, Phys. Rev. Lett. **105**, 137202 (2010).
[25] S. Miyahara and N. Furukawa, J. Phys. Soc. Jpn. **80**, 073708 (2011).

[26] K. Penc, J. Romhányi, T. Rõõm, U. Nagel, A. Antal, T. Fehér, A. Jánossy, H. Engelkamp, H. Murakawa, Y. Tokura, D. Szaller, S. Bordács, and I. Kézsmárki, Phys. Rev. Lett. **108**, 257203 (2012).
[27] T. Arima, J. Phys. Soc. Jpn. **76**, 073702 (2007).
[28] K. Yamauchi, P. Barone, and S. Picozzi, Phys. Rev. B **84**, 165137 (2011).
[29] M. Akaki, H. Iwamoto, T. Kihara, M. Tokunaga, and H. Kuwahara, Phys. Rev. B **86**, 060413(R) (2012).
[30] M. Akaki, D. Yoshizawa, A. Okutani, T. Kida, J. Romhányi, K. Penc, and M. Hagiwara, Phys. Rev. B **96**, 214406 (2017).
[31] Y. Iguchi, Y. Nii, M. Kawano, H. Murakawa, N. Hanasaki, and Y. Onose, Phys. Rev. B **98**, 064416 (2018).
[32] The number of the domains is determined by the order of the factor group $S_4 \cong P\bar{4}2_1m1'/P2_1'2_12'$, which also transforms the domain states among each other.
[33] I. Kézsmárki, U. Nagel, S. Bordács, R. S. Fishman, J. H. Lee, H. T. Yi, S.-W. Cheong, and T. Rõõm, Phys. Rev. Lett. **115**, 127203 (2015).
[34] See Supplemental Material at http://link.aps.org/supplemental/10.1103/PhysRevLett.127.157201 showing that NDD has the same magnitude after ME annealing.
[35] J. Viirok, U. Nagel, T. Rõõm, D. G. Farkas, P. Balla, D. Szaller, V. Kocsis, Y. Tokunaga, Y. Taguchi, Y. Tokura, B. Bernáth, D. L. Kamenskyi, I. Kézsmárki, S. Bordács, and K. Penc, Phys. Rev. B **99**, 014410 (2019).
[36] T. Nakajima, Y. Tokunaga, V. Kocsis, Y. Taguchi, Y. Tokura, and T.-h. Arima, Phys. Rev. Lett. **114**, 067201 (2015).
[37] P. C. Hohenberg and W. F. Brinkman, Phys. Rev. B **10**, 128 (1974).
[38] S. Kimura, M. Matsumoto, and H. Tanaka, Phys. Rev. Lett. **124**, 217401 (2020).